

Prompt Highlighter: Interactive Control for Multi-Modal LLMs

Yuechen Zhang¹ Shengju Qian¹ Bohao Peng¹ Shu Liu² Jiaya Jia^{1,2}
¹The Chinese University of Hong Kong ²SmartMore

<https://github.com/dvlab-research/Prompt-Highlighter>

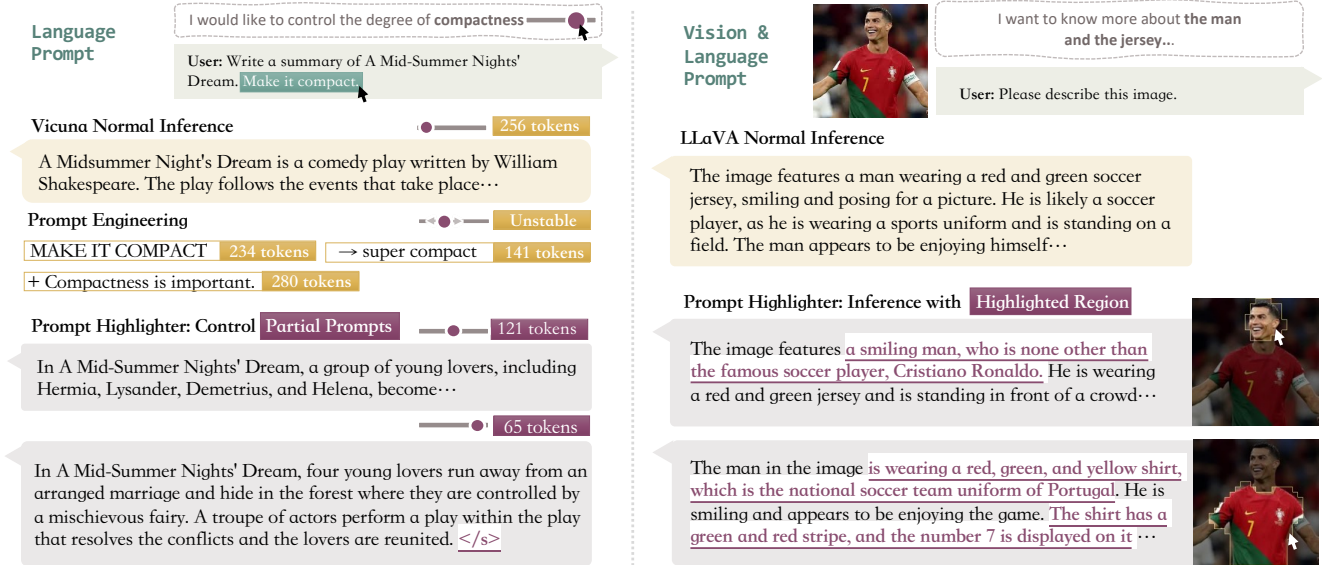


Figure 1. Prompt Highlighter facilitates token-level user interactions for customized generation, compatible with both LLMs and VLMs. Compared with vanilla inference and prompt engineering, the context-highlighted inference provided by our method offers controllable generations and produces customized results. Outputs correlated with the highlighted parts are underlined.

Abstract

This study targets a critical aspect of multi-modal LLMs' (LLMs&VLMs) inference: explicit controllable text generation. Multi-modal LLMs empower multi-modality understanding with the capability of semantic generation yet bring less explainability and heavier reliance on prompt contents due to their autoregressive generative nature. While manipulating prompt formats could improve outputs, designing specific and precise prompts per task can be challenging and ineffective. To tackle this issue, we introduce a novel inference method, Prompt Highlighter, which enables users to highlight specific prompt spans to interactively control the focus during generation. Motivated by the classifier-free diffusion guidance, we form regular and unconditional context pairs based on highlighted tokens, demonstrating that the autoregressive generation in models can be guided in a classifier-free way. Notably, we find that, during inference, guiding the models with highlighted tokens through the attention weights leads to more desired outputs. Our approach is compatible with current LLMs

and VLMs, achieving impressive customized generation results without training. Experiments confirm its effectiveness in focusing on input contexts and generating reliable content. Without tuning on LLaVA-v1.5, our method secured 70.7 in the MMBench test and 1552.5 in MME-perception.

1. Introduction

Large Language Models (LLMs) have driven significant progress in a multitude of natural language processing tasks [1–9]. Further advancements have been achieved by extending these models to handle vision-language tasks [10–15] through visual-language alignment and instruction tuning. These efforts have led to the development of Vision Language Models (VLMs), which can generate text based on multi-modal inputs. Due to its autoregressive nature, the typical generation process in LLMs and VLMs (multi-modal LLMs) is primarily conditioned on input contexts. Prompt engineering [16–19] has emerged as a common interaction mechanism between humans and language models, where diverse formats and content of prompts are employed to steer the generation towards de-

sired outcomes. However, prompt engineering often relies on empirical intuition and requires careful design of the context, making it less accessible for non-experts. As illustrated in the left part of Fig. 1, even the meticulously crafted prompts, which convey the concept of ‘compactness’ clearly, can lead to unpredictable outputs that fail to meet the requirements.

Instead of manipulating prompt-level contexts (*i.e.*, prompt engineering) to control LMs’ generation process, we propose a novel inference approach, Prompt Highlighter, that enables token-level user interactions for personalized generations. Our method allows users to interact with multi-modal LLMs in a manner analogous to applying a highlighter tool on the input context in the text editor, enabling users to emphasize desired parts by highlighting them.

This highlighting mechanism is achieved by constructing a regular and unconditional input context pair with different textual embeddings in the highlighted tokens. Subsequently, we can adjust the model’s focus on the highlighted components by employing the classifier-free guidance [20–22] on predicted token probabilities. Moreover, by probing cross-token attention maps, we discover a robust correlation between attention scores and the semantic significance of tokens. This suggests that, in the autoregressive generation process of language models, the semantic relationship between tokens can be represented to a certain extent by their attention scores. Building on this insight, we introduce an attention activation strategy that adjusts the attention weights associated with a highlighted part. Specifically, Prompt Highlighter employs an adjusted attention mask to reweight corresponding attention scores, enabling a more focused generation on highlighted parts.

As illustrated in Fig. 1, compared to vanilla inference, our highlighted inference can guide the generation process to produce controllable results that align more closely with user needs. Prompt Highlighter is compatible with mainstream transformer-based multi-modal LLMs. This compatibility encompasses VLMs that use precise patch-wise visual token mapping, such as LLaVA [10, 23, 24], as well as methods that employ implicit query-based visual token mapping, like those based on Q-Former [11, 13–15]. This novel interaction paradigm with highlighted sections during the generation process goes beyond what prompt engineering can offer.

We further demonstrate the effectiveness of Prompt Highlighter by evaluating it using comprehensive multi-modal benchmarks. We verify that directly highlighting the full image context in VLMs can significantly improve the quality of generated image captions [25] and question-answering results. Specifically, our method can effectively mitigate the model’s propensity to hallucinate by guiding its focus toward reliable contexts, thereby enhancing overall performance. Notably, without additional training, our

method improves the performance of the baseline LLaVA-v1.5, securing 2nd place in both MMBench [26] and MME-perception [27] leaderboards.

Our contributions can be summarized as follows: (1) We pioneer the exploration of fine-grained human-model interactions in multi-modal LLMs, proposing a plug-and-play pipeline that enables token-level user interactions for controllable generation. (2) We conduct extensive experiments on comprehensive benchmarks, demonstrating that our method significantly enhances the overall performance.

2. Related Works

2.1. Multi-Modal LLMs

Recent Large Language Models (LLMs) [1, 7–9, 28–30] play a significant role in natural language processing tasks, particularly in language generation and question answering. Building upon these pre-trained language models, Vision-Language Models (VLMs) [10, 11, 13–15, 31] further introduce the alignment between vision and language modalities by leveraging extensive training on image-caption pairs or image-question conversations. There are two prevalent methods for aligning vision and verbiage modalities. The first method, exemplified by LLaVA [10], directly maps image patches to tokens using a projector, establishing a one-to-one correspondence. The second method, represented by models like BLIP2 [13, 32], employs a Query Transformer (Q-Former) after getting image features to establish a non-uniform patch-token mapping. These methods use learnable queries to get compressed image features, yielding visual tokens rich with semantic information.

2.2. Interactions with Multi-Modal LLMs

Prompt engineering and interactions. Based on the autoregressive property of LLMs, users aim to control the generation results by modifying the input contexts. This largely determines the test-time interactions with LLMs, primarily executed through prompt engineering. Representative methods such as CoT [17] introduce demonstrations in the context to enhance reasoning ability. Other multi-branch designs like ToT and GoT [16, 18, 19, 33, 34] have been proposed for rich and reliable context generation and self-checking. Aside from prompt engineering, human-model interactions have not been extensively explored in VLMs. Methods like Kosmos-2 [31], LLaVAInteractive [35], LISA [36], and AlphaCLIP [37] enable grounding perception tasks such as detection, segmentation, caption, and image editing through interaction with LLMs. These task-oriented interactions require additional data collection and task-specific tuning. In contrast, Prompt Highlighter is plug-and-play for general text generation in pre-trained models.

Classifier-free guidance and controllable generation. Classifier-Free Guidance (CFG) [20] enables a control on Diffusion Models’ generation process without a conven-

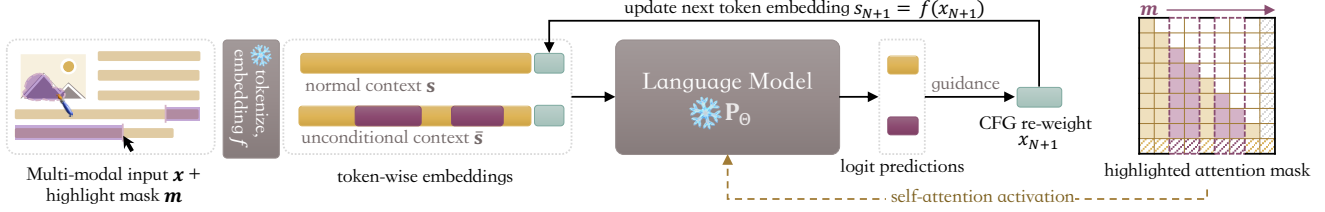


Figure 2. An abstract pipeline of Prompt Highlighter. Users can control the focus of generation by marking out specific image regions or text spans. Then a token-level mask \mathbf{m} is created to guide the language model’s inference.

tional classifier. Specifically, CFG’s step-wise sampling allows users to employ a negative prompt within the unconditional branch, effectively guiding the generation away from harmful distributions. This approach has been extended to language models by LLM-CFG [21], allowing a controllable text generation and improved performance. However, LLM-CFG still requires a pair-wise prompt design and does not support partial token-level reweighting within the context, which is vital for controlling VLM’s generation. Besides, methods in Diffusion Models [38, 39] achieve fine-grained control over image generation using text prompts by emphasizing areas within cross-attention maps. Fine-grained control over autoregressive generation in LLMs and VLMs is still challenging. Later concurrent works CRG and MARINE [40, 41], adopt CFG in VLMs for grounding and mitigating hallucination, but employ a different design for positive-negative pairs compared to our approach.

3. Prompt Highlighter

An overview of Prompt Highlighter is presented in Fig. 2. Given a pre-trained generative model \mathbf{P}_Θ , we first extract the input tokens from the text and the input image, forming the prompt context \mathbf{x} . Subsequently, by marking out specific image regions or text spans, user creates a token-level binary mask \mathbf{m} to highlight specific tokens. Prompt Highlighter then generates the output sequence \mathbf{y} using the two-branch condition based on \mathbf{m} autoregressively. The following section will delve into the specifics of our method.

3.1. Token-Level Highlight Guidance

In conditioned Diffusion Models [42], given a noisy image x and a class condition c , the model predicts probability likelihood $\hat{\mathbf{P}}$, for the conditioned step-wise sample, $\hat{\mathbf{P}}_\Theta(x|c) \propto \mathbf{P}_\Theta(x) \cdot \mathbf{P}_\Phi(c|x)^\gamma$. Here, \mathbf{P}_Φ is a classifier, and γ is the guidance strength controlling the weight of likelihood on c . Ho et al. [20] observed that guidance can be offered without a classifier. Applying the Bayes rule, $\mathbf{P}_\Theta(c|x) \propto \mathbf{P}_\Theta(x|c)/\mathbf{P}_\Theta(x)$, the sampling process of the Classifier-Free Guidance (CFG) can be expressed as

$$\hat{\mathbf{P}}_\Theta(x|c) \propto \mathbf{P}_\Theta(x|c)^\gamma / \mathbf{P}_\Theta(x)^{\gamma-1}, \quad (1)$$

$$\log \hat{\mathbf{P}}_\Theta(\epsilon_t|x_{t+1}, c) = \gamma \log \mathbf{P}_\Theta(\epsilon_t|x_{t+1}, c) - (\gamma - 1) \log \mathbf{P}_\Theta(\epsilon_t|x_{t+1}), \quad (2)$$

in which ϵ_t is the noise prediction conditioned on the previous output x_{t+1} and the text condition c . LLM-CFG [21] extended this property to autoregressive language models. Given a sequence of N tokens $\mathbf{x} = \{x_1, \dots, x_N\}$, the likelihood of predicting the entire sequence can be expressed as $\mathbf{P}_\Theta(\mathbf{x}) = \prod_i^N \mathbf{P}_\Theta(x_i|x_{j<i})$. The model samples each subsequent token from the conditional probability distribution. Based on Eq. (1), the CFG sampling on the language model can be denoted as

$$\hat{\mathbf{P}}_\Theta(\mathbf{x}|c) \propto \frac{\mathbf{P}_\Theta(\mathbf{x}|c)^\gamma}{\mathbf{P}_\Theta(\mathbf{x})^{\gamma-1}} \propto \prod_{i=1}^N \frac{\mathbf{P}_\Theta(x_i|x_{j<i}, c)^\gamma}{\mathbf{P}_\Theta(x_i|x_{j<i})^{\gamma-1}}. \quad (3)$$

Similar to the transaction from Eq. (1) to Eq. (2), the likelihood in LLM is represented as the next-token classification probability. Thus next token’s logit prediction $\mathbb{P}x_i = \log \hat{\mathbf{P}}_\Theta(x_i|x_{j<i}, c)$ is

$$\mathbb{P}x_i = \gamma \log \mathbf{P}_\Theta(x_i|x_{j<i}, c) - (\gamma - 1) \log \mathbf{P}_\Theta(x_i|x_{j<i}). \quad (4)$$

The formulation in Eqs. (3) and (4) offers a paradigm for controllable generation in LLMs [21], with the guidance strength γ controls the degree of generation focus. Notably, the effectiveness of this guidance depends on the careful design of the conditional prompt c , which should be naturally formed as a complete phrase or sentence to retain its semantic meaning. Prompt Highlighter extends CFG control in language models in a more generalized manner. The user’s selection on the context \mathbf{x} is converted into a token-level binary highlight mask $\mathbf{m} = \{m_1, \dots, m_N\}$. We define $m_i = 1$ if the i -th token x_i is highlighted, and $m_i = 0$ otherwise. This mask constructs a two-branch condition: the normal and the unconditional contexts. The normal context operates in the same manner as in vanilla inference. Meanwhile, the unconditional context $\bar{\mathbf{s}}$ is derived from the normal conditional context $\mathbf{s} = \{s_1, \dots, s_N\}$ within the textual embedding space through a token-wise scaling,

$$\bar{s}_i = (\alpha - 1)m_i \cdot f(x_i) + f(x_i), \quad (5)$$

where α is the scaling factor and $f(\cdot)$ is the token-to-embedding function, *i.e.*, $s_i = f(x_i)$. We empirically set a small rescale α (*e.g.*, 0.01) that can ensure a normal inference while ignoring the highlighted part. Then, based on the two-branch condition $(\mathbf{s}, \bar{\mathbf{s}})$, we can define the i -th token sampling process of the token-level highlight guidance as



Figure 3. Visualizing attention maps. **Left:** A segment of the attention map between the generated tokens and the input requirement prompt: “... fix the grammar and keep LaTeX format, make it compact...”. Some representative tokens are marked for reference. **Right:** Query-based token mapping. This shows the attention score on 32 queries in the first cross-attention layer of the Q-Former.

$$\log \hat{\mathbf{P}}_{\Theta}(x_i | s_{j < i}) = \gamma \log \mathbf{P}_{\Theta}(x_i | s_{j < i}) - (\gamma - 1) \log \mathbf{P}_{\Theta}(x_i | \bar{s}_{j < i}). \quad (6)$$

Compared with Eq. (4), the additional conditional context c is naturally incorporated as the difference between \mathbf{s} and $\bar{\mathbf{s}}$. This arrangement provides users with the flexibility to control the in-line requirements. After the i -th token is predicted, the highlight mask \mathbf{m} and contexts $\mathbf{s}, \bar{\mathbf{s}}$ are updated by appending $m_i = 0$ and $s_i = \bar{s}_i = f(x_i)$, respectively. The generation process is terminated when the end token $\langle /s \rangle$ is predicted.

3.2. Attention Activation

The token-level highlight guidance anchors the generative process with a token-wise logit reweighting. However, its effectiveness may diminish when facing long and complex input contexts with few highlighted tokens, making it difficult to distinguish \mathbf{s} and $\bar{\mathbf{s}}$. To further investigate token-wise correlations and their impact on generation results, we exclude sink tokens that dominate the attention score [43] and visualize cross-token self-attention score maps during inference. For instance, in the left of Fig. 3, pivotal tokens form a band-like pattern on the attention map, drawing attention from nearly all following tokens. This pattern endures with changes in the model’s layer number or attention heads, suggesting the attention mechanism’s consistency and robustness in well pre-trained LLMs [7, 8]. Meanwhile, it implies that attention scores within the model can represent the semantic correlation between tokens.

When addressing diverse requirements, LLMs need to balance attention among multiple tokens. For instance, as seen in Fig. 3 (left), as one of the requirements in the prompt, ‘compactness’ might not get enough attention during the generation process, resulting in an output that is less compact than expected. Given the direct correlation observed between attention and tokens, we propose an attention activation strategy to activate the attention scores on highlighted tokens within the attention mechanism. This strategy can effectively steer the model’s focus towards or away from specific tokens, allowing for more nuanced and precise control over the output. We reformulate the model inference function in Eq. (6) to a mask-conditioned one

$\tilde{\mathbf{P}}_{\Theta}(x_i | s_{j < i}, \mathbf{m})$. In each of its self-attention layers, let \mathbf{k}_i represent the i -th column vector of the query-key multiplied attention score matrix in one attention head. The activated attention score h_i **in the normal context branch** is defined as

$$h_i = \log(\beta) \cdot m_i + k_i. \quad (7)$$

Then, the attention probability p_i is calculated as

$$p_i = \frac{\exp(h_i)}{\sum_{j=1}^N \exp(h_j)} = \frac{\beta^{m_i} \cdot \exp(k_i)}{\sum_{j=1}^N \beta^{m_j} \cdot \exp(k_j)}. \quad (8)$$

This mechanism defines the activation scaling factor as β . **For the unconditional branch**, the attention score is deactivated by using a scaled negative mask in the inference $\tilde{\mathbf{P}}_{\Theta}(x_i | \bar{s}_{j < i}, -\delta \mathbf{m})$. Eq. (8) presents a SoftMax probability $p_i = \text{softmax}(h_i)$ on the activated scores, with a consistent β^{m_i} -times probability augmentation on highlighted tokens. The attention activation operates under the assumption that users cannot highlight dominant ‘sink’ tokens as explored in [43]. Consequently, the attention activation will not catastrophically impair the model’s fundamental generative capabilities during the inference.

3.3. Highlighting Visual Tokens

Methods for highlighting visual tokens can be classified into two categories based on the type of token mapping involved, as discussed in Sec. 2.1. In direct token mapping, such as in LLaVA [10], the highlighting of visual tokens is straightforward. Image patch-level feature forms the sequential visual contexts \mathbf{s}^{im} . This enables a natural patch-level scaling on embeddings in Sec. 3.1 and attention activation introduced in Sec. 3.2.

In contrast, the scenario becomes more complex with query-based token mapping. For example, in works like BLIP-2 [11, 13, 14], the image feature is transformed into a unified set of few learnable queries \mathbf{q} via Q-Former, which are then input into LLMs as textual embeddings. This process obscures the direct correlation between image patches and input tokens, as demonstrated in the example on the right side of Fig. 3. To address this challenge, we leverage the fact that the Q-Former itself is a Transformer model to perform the token highlighting directly inside it. First, we

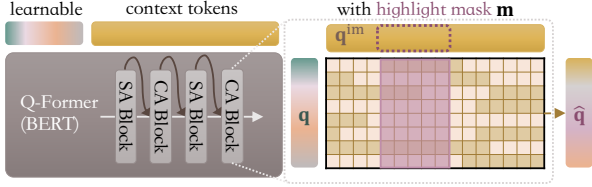


Figure 4. Highlighting visual tokens with Q-Former-based methods. In comparison with vanilla inference, we augment the learnable queries \mathbf{q} by activating corresponding attention weights in the Cross-Attention (CA) blocks.

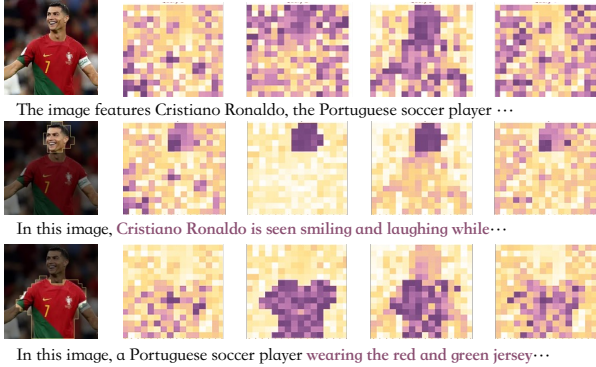


Figure 5. Attention scores in the first four queries of the Q-Former. Each row shows a different user selection and text output.

adopt the embedding rescale in Eq. (5) on the patch-wise image feature and use the output queries from the Q-Former to form the image context pair $(\mathbf{s}^{\text{im}}, \bar{\mathbf{s}}^{\text{im}})$. Then, by activating attention scores within the corresponding patch-wise user-selection mask \mathbf{m} in Q-Former’s cross-attention layers, we can effectively steer the model to adjust its focus. This process is depicted in Fig. 4. In the Q-Former model, cross attention is calculated across the learnable query $\mathbf{q} = \{q_1, \dots, q_M\}$ and the image feature $\mathbf{q}^{\text{im}} = \{q_1^{\text{im}}, \dots, q_N^{\text{im}}\}$. We then activate the attention score corresponding to the mask \mathbf{m} within the cross-attention map. It can be expressed using a formulation similar to Eq. (7),

$$\hat{\mathbf{q}} = \text{softmax} \left((\log(\beta) \cdot \mathbf{w} + QK^\top) / \sqrt{d_k} \right) V, \quad (9)$$

where $Q = f_q(\mathbf{q})$, $K = f_k(\mathbf{q}^{\text{im}})$, and $V = f_v(\mathbf{q}^{\text{im}})$ represent the transformed QKV vectors in the cross attention with projections $f_{(\cdot)}$, and d_k denotes the dimension of K . As a variation of the activation process in Eqs. (7) and (8), \mathbf{w} is a resized version of \mathbf{m} , expanding dimension from N to (H, M, N) , where H denotes the number of attention heads. We illustrate the variations in attention scores with changing input masks in Fig. 5. Attention score maps show attention concentrations in masked areas. This guides the model’s focus towards specific visual elements, leading to various generation outputs.

4. Experiments

4.1. Implementation Details

Pre-trained models. Prompt Highlighter can be applied to a variety of general frameworks. For LLMs, we employ the LLaMA model architecture [7] and utilize Vicuna-13B v1.1 [8] as the test model. For VLMs, experiments are done on one direct token mapping model LLaVA-13B [10, 23] and one query-based mapping model InstructBLIP-Vicuna-13B [15]. We adopt the LLaVA-v1.5 13B model [23] in quantitative evaluations. All experiments are conducted on a single NVIDIA-A800 GPU.

Hyper-parameters. The following parameter configurations are constant throughout almost all examples. In the highlight guidance, we set the guidance strength $\gamma = 1.3$ in Eq. (6), and the scaling parameter α in Eq. (5) is set to 0.01. In attention activation, we accommodate the diverse feature domains across different models by setting $\beta = 2.0$ in Eq. (7) and $\beta = 20.0$ in Eq. (9). The scale factor δ in Eq. (7) is set to satisfy $\delta \mathbf{m} = (\log(\beta) + 2)\mathbf{m}$.

Inference. During user interactions, if the text range selected by the user does not align perfectly with the tokens from the tokenizer, we adjust the start or end selection position to ensure that the selected range is fully encompassed. For images, the input mask is downsampled to a patch-wise binary mask based on the input image. The size depends on the visual encoder’s patch size (e.g., CLIP). In the autoregressive generation process, we employ a greedy search and cache prior KV values across layers.

4.2. Applications and Comparisons

Partial context highlighting is a fundamental application of Prompt Highlighter, utilized in scenarios where the emphasis is required on specific spans of the context. As shown in Figs. 1 and 6, our method enables users to guide the model’s attention toward relevant parts of the input by highlighting them. It enhances the focus and relevance of the generated output across a range of diverse frameworks [8, 10, 15], making results align more precisely with user-selected tokens. It’s worth noting that the examples in Fig. 6 can not be achieved by LLM-CFG [21], as it requires a prompt design that has complete sentences or images. This approach proves particularly useful in tasks such as content summarization and interactive conversations.

Generation control. As demonstrated in Fig. 1, we can further control the degree of correlation to the highlighted part in text generation. Users can manipulate the model’s output dynamically by adjusting the highlight guidance strength γ in Eq. (6). This capability can prove advantageous in a variety of tasks, ranging from generating descriptive captions for images to creating customized responses in conversational agents.

Reliable description. When carrying out long text genera-



Figure 6. Partial context highlighter. When given user input, vanilla inference might lead to unfocused generations. Our context-highlighted inference can faithfully capture the content of the highlighted part. The highlighted sections in each case are marked with circled indices in the image. Outputs correlated with the highlighted parts are underlined.

tion tasks, every predicted token interacts with all previous content, including the newly generated contexts, to gather information. This may lead to a gradual divergence and loss of attention between the generated tokens and the input context, causing the model to hallucinate. We address this issue by highlighting all user input condition tokens, thereby guiding the generated content to align more closely with the input context. This approach is particularly vital for descriptive tasks, such as generating image captions. We demonstrate this in Fig. 7. Our method can generate more accurate and detailed descriptions. Moreover, when the generated description is fed into an image generation model like DALLE-3 [44], our method demonstrates its advantages in facilitating image-text alignment.

4.3. Quantitative Evaluation

General VLM benchmarks. In Tab. 1, we evaluate our method on common comprehensive Vision-Language

benchmarks, MME [27] and MMBench [26]. Prompt Highlighter on LLaVA-v1.5 demonstrates a consistent performance improvement compared to well-trained models by designating the entire image as the highlighted part in the input context. Notably, though these benchmarks primarily assess overall performance with single-token generation and are not designed for user interactions, we still get a competitive place in both MMBench and MME perception. Additionally, further benchmarking with different hyper-parameter selection validates our performance enhancements with LLaVA-v1.5 13B, as evidenced by gains on POPE (85.9 - 87.8, +1.9), MMB^{CN} (63.4 - 64.0, +0.6), and SQA^I (71.6 - 72.4, +0.8). With LLaVA-NeXT-34B [45], we achieve a SOTA performance on MMB^{test} with 81.3.

Reliable description. We then evaluate the reliability of image captions generated by our method. In this case, we utilized the reference-free metric CLIP Score [48], ex-



Figure 7. Results when highlighting all input contexts. Given user input , vanilla inference might lead to hallucinations. In contrast, context-highlighted inference can accurately capture the content of the image. We further feed descriptions into DALLE-3 [44] (shown on the right) to provide a visually apparent difference. The CLIP-Similarity [30] with the input image is reported for each generated image.

method	MME	MMB _{dev}	MMB _{test}	PoPE
QWen-VL-Chat [46]	1487.5	60.6	61.8	-
mPLUG-Owl-2 [14]	1540.2	64.5	66.0	-
LLaVA-v1.5 [23]	1531.3	67.7	67.0	85.9
Prompt Highlighter	1552.5 ⁺²¹	69.7 ^{+2.0}	69.5 ^{+2.5}	87.8 ^{+1.9}

Table 1. Evaluations on comprehensive VLM benchmarks, including MME Perception [27] and MMBench (MMB) [26].

method	S-CLIP	text → image		image → text	
		R@1	R@5	R@1	R@5
FuseCap [47]	0.785	37.2	62.3	47.7	72.3
CoCa-CFG [22]	0.808	44.6	71.7	-	-
LLaVA-v1.5 [23]	0.809	36.6	62.2	50.7	76.4
Prompt Highlighter	0.829	45.2	71.7	62.2	85.0

Table 2. CLIP-based reference-free image caption evaluation conducted on the MSCOCO [25].

pressed as $S\text{-CLIP} = 2.5 \cdot \max(\cos(v, c), 0)$, to evaluate the embedding similarity between the image v and the generated caption c . We also report the text \leftrightarrow image retrieval recall R@1, R@5 in the CLIP embedding space. As demonstrated in Tab. 2, on the MSCOCO Karpaty test set [25], our method shows a state-of-the-art CLIP score when compared to recent competitive caption-focused methods [22, 47]. Our results exhibit significant advantages across all metrics compared to the baseline.

User study. We conduct a user study to assess the usability

and effectiveness of our method. This study asks participants to rank generation results across five tasks (image captioning, image/text partial highlight generation, text for image generation, and image understanding). Compared with the original inference baselines, the collected 255 valid preference results indicated that **77.3%** of users found Prompt Highlighter to generate more correlated results and be beneficial in accomplishing the task objectives.

More details about the quantitative evaluation can be found in Appendix A.2.

4.4. Ablation Study

Module-wise ablation. In Tab. 3, we systematically conduct an ablation study by removing each module of Prompt Highlighter and noting the performance change in MME and MMBench_{dev}. The results revealed that removing the attention activation module led to the most considerable performance reduction, and combining the highlight guidance and attention activation significantly improves the overall performance.

Hyper-parameters. In Tab. 4, we explore the impact of three scaling parameters (α, β, γ) in Eqs. (5) to (7) for highlight control on the performance of our method. We observed a trade-off between higher concentration (higher β and γ) and general vision-language understanding ability.

settings	Guidance	Attention	MME	MMB _{dev}
baseline (our impl.)			1528.7	67.7
w/ Guidance	✓		1531.1	68.5
w/ Attention		✓	1537.2	69.5
Full pipeline	✓	✓	1552.5	69.7

Table 3. A module-wise ablation study.

α (in Eq. (5))	0.0	0.01	0.1	1.0
(α , 2.0, 1.3)	1517.6	1552.5	1522.3	<u>1524.2</u>
β (in Eq. (7))	1.0	2.0	3.0	4.0
(0.01, β , 1.3)	1527.2	1552.5	<u>1537.3</u>	1535.7
γ (in Eq. (6))	1.0	1.3	1.5	2.0
(0.01, 2.0, γ)	<u>1537.2</u>	1552.5	1532.6	1524.0

Table 4. Hyper-parameter ablation on MME. We probe for the most suitable value for one of the combinations in (α , β , γ).

method	token/s \uparrow	memory (MB) \downarrow	S-CLIP \uparrow
Baseline	6.67	16231	0.809
Baseline beam=2	5.97	18537	0.807
Prompt Highlighter	5.95	17373	0.829

Table 5. Evaluation on inference speed and GPU memory. The memory is dominated by the model weight, consuming 13971 MB.

4.5. Discussions

Prediction control by CFG. Given that our highlight guidance operates on the predicted token probability, similar to LLM-CFG [21], we further investigate the semantic-level distinctions in normal and unconditional branches. This is visualized through an example of token prediction in Fig. 8. When the embeddings associated with the highlighted tokens are perturbed, the unconditional-context branch tends to predict unrelated to the highlighted parts. This, in turn, enables the rectification of responses in text-generation tasks.

Attention activation. To confirm that the attention activation operates as anticipated, we not only visualize the activated attention scores corresponding to different regions in Fig. 5, but we also demonstrate its effectiveness using 500 attention maps from the caption experiment in Fig. 9. Firstly, we validate the band-like pattern property discussed in Sec. 3.2, by comparing the vertical and horizontal gradients. We observed a significant gradient gap with $G_x > G_y$ in all 500 cases. Given this property, the attention activation can capture a higher attention probability p , as defined in Eq. (8), from the given contexts. This attention contribution plotted in Fig. 9 is denoted as $\sum_{m_i=1}(p_i)/\sum_{j<i}(p_j)$. Consequently, attention activation leads to results that adhere more closely to the input context.

Limitations and future work. While our approach introduces a novel method for controlling generation in multi-modal LLMs, it has certain limitations: (a). *Additional computations:* Our method requires an extra decoding branch, which brings additional computational overhead and GPU memory requirements. However, these additional

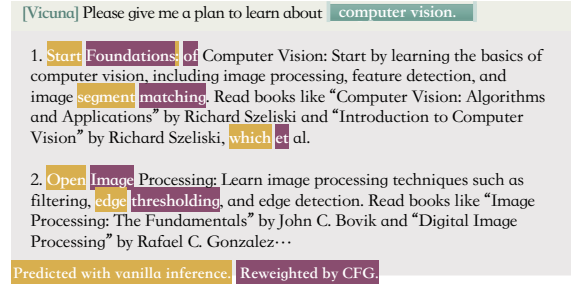


Figure 8. An example of token changed with CFG.

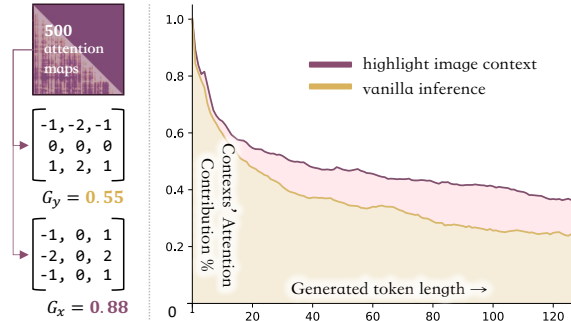


Figure 9. *Left:* A simple verification of the vertical band-like pattern in the attention map, with a report on the gradient summation. *Right:* Following [49], we present a visualization displaying the average contribution of context’s attention during generation.

loads are marginal and acceptable with the batched inference. We validate this by the caption experiment in Tab. 5. (b). *Dependence on base model:* Content generation quality is tied to the base model’s capabilities, which may result in over-emphasis or miss-emphasis on highlighted parts when using poorly-trained base models.

One direction for future work will be to create a more intuitive highlighting scheme. We also aim to extend our method to support a greater variety of interactions.

5. Conclusion

We introduce Prompt Highlighter, a novel paradigm for user-model interactions in multi-modal LLMs, offering output control through a token-level highlighting mechanism. This approach, requiring no extra training, competes well on standard benchmarks and provides reliable generation outputs by merely highlighting input context. Further, diverse applications demonstrate its intuitive usability and effectiveness in enhancing control over the generation process. This work represents a promising direction for enhancing user control in multi-modal LLMs, and we anticipate it will inspire further research.

Acknowledgement This work was supported in part by the Research Grants Council under the Areas of Excellence scheme grant AoE/E-601/22-R and the Shenzhen Science and Technology Program under No. KQTD20210811090149095.

Appendix Contents

A. Experiment Details	9
A.1. Workflow of the Prompt Highlighter	9
A.2. Quantitative Evaluation	9
A.2.1 VLM Benchmarks	9
A.2.2 Reliable Descriptions	10
A.2.3 User Study	10
A.3. Attention Map Visualization	10
A.4. Limitation Analysis	11
A.4.1 Speed and Memory	11
A.4.2 Constrained by the Base-Model	12
B. Additional Discussions	12
B.1. Compare with LLM-CFG	12
B.2. Compare with other Highlight Methods	13
B.3. Highlighting the Whole Image.	13
C. Showcases	13
C.1. More Visual Results	13
C.2. Multi-Round Interactive Conversation	13

A. Experiment Details

A.1. Workflow of the Prompt Highlighter

For a more comprehensive understanding of the method part of Prompt Highlighter, we provide pseudo-code algorithmic workflows in Algorithm 1 and Algorithm 2. In this context, the attention activation outlined in Algorithm 2 acts as the modified forward function in all Self-Attention layers during the multi-modal LLMs’ inference $\tilde{\mathbf{P}}_{\Theta}(x_{\eta}|\mathbf{s}, \mathbf{m})$, as discussed in Sec. 3.2 and illustrated in Algorithm 1.

Algorithm 1 Highlighted Guidance Control

Require: Pre-trained LLM or VLM decoder \mathbf{P}_{Θ} , input multi-modal tokens \mathbf{x} , binary highlight mask \mathbf{m} , guidance strength γ , and scaling factor α, δ

- 1: Initialize token sequence $\mathbf{x} = \{x_1, \dots, x_N\}$
- 2: Initialize conditional embedding $\mathbf{s} = f(\mathbf{x})$ and unconditional embedding $\bar{\mathbf{s}}$ as $\bar{\mathbf{s}} = (\alpha - 1)\mathbf{m} \cdot f(\mathbf{x}) + f(\mathbf{x})$ (Eq. (5)).
- 3: Initialize current token index $\eta = N$, output token sequence $\mathbf{y} = []$
- 4: **while** x_{η} is not $\langle /s \rangle$ **do**
- 5: Calculate the greedy decoded prediction x_{η} in Eq. (6):
- 6: $x_{\eta+1} = \operatorname{argmax}(\gamma \log \tilde{\mathbf{P}}_{\Theta}(x_{\eta+1}|\mathbf{s}, \mathbf{m}) - (\gamma - 1) \log \tilde{\mathbf{P}}_{\Theta}(x_{\eta+1}|\bar{\mathbf{s}}, -\delta\mathbf{m}))$
- 7: Update output sequence:
- 8: $\mathbf{y}.\operatorname{append}(\mathbf{P}_{\Theta}.\operatorname{tokenizer}.\operatorname{decode}(x_{\eta+1}))$
- 9: Update next token embedding and mask:
- 10: $s_{\eta+1} = \bar{s}_{\eta+1} = f(x_{\eta+1}), m_{\eta+1} = 0, \eta = \eta + 1$
- 11: **end while**
- 12: **return** Output sequence \mathbf{y}

Algorithm 2 Attention Activation in Self-Attention Layer.

For simplicity, we demonstrate with single-head attention.

Require: Input hidden state $\mathbf{q} = \{q_1, \dots, q_{\eta-1}\}$ and vanilla attention mask \mathbf{m}_{attn} , highlight mask \mathbf{m} , Scaling factor β , Self-Attention Module $M_{\text{SA}} \subset \tilde{\mathbf{P}}_{\Theta}$.

- 1: $(Q, K, V) = M_{\text{SA}}.\operatorname{proj_qkv}(\mathbf{q})$
- 2: Calculate the attention score map:
- 3: $\mathbf{k} = Q@K^{\top} + \mathbf{m}_{\text{attn}}$
- 4: Initialized the highlighted attention mask:
- 5: $\mathbf{w} = \mathbf{m}.\operatorname{expand_as}(\mathbf{k})$
- 6: Activate score via attention map (Eqs. (7) and (9)):
- 7: $\mathbf{h} = \log(\beta)\mathbf{w} + \mathbf{k}$
- 8: Then complete the remaining operations in self-attention:
- 9: $\mathbf{p} = \operatorname{softmax}(\mathbf{h})$
- 10: **return** $\mathbf{q}_{\text{out}} = M_{\text{SA}}.\operatorname{proj_out}(\mathbf{p}@V)$

A.2. Quantitative Evaluation

A.2.1 VLM Benchmarks

We use the same prompts and test scripts for our benchmark tests as those in the LLaVA-v1.5 codebase [23]. The only difference is our highlighting of the image context in the inputs (*i.e.*, $m_i = 1$ when $s_i \in \mathbf{s}^{\text{im}}$). We adopt softmax, instead of log softmax used in the multiple-token prediction tasks, as the token probability rescale function. As discussed in Sec. 4.4, we observe slight variations in results across different test sets based on the parameters of attention activation. In Tab. 7, we showcase the impact of changes in the β value on the benchmark tests. Our method still achieves the second rank on the current MMBenchmark leaderboard, even when using a uniform parameter of $\beta = 2.0$.

We adopt the MME and MMBench datasets because they offer comprehensive evaluations of VLMs across multiple dimensions and feature over 10K of VQA questions. This makes them ideal for assessing the overall competency of Vision-Language Models. We present a detailed evaluation result of MMBench in Tab. 6. With the same pre-trained weight as LLaVA-v1.5, our training-free method consistently outperforms the baseline across nearly all evaluation dimensions. Given that our approach is compatible with VLM frameworks that use token-level embedding input and a Transformer-based language decoder, it positions the Prompt Highlighter as a **training-free plugin** for integrating context-highlighting abilities into these models. We further evaluate the MMBench benchmark using the current state-of-the-art model, InternLM-VLComposer [32]. Our method demonstrated a performance improvement, increasing the SOTA performance from 74.8 to 75.3 in the dev split with this representative Q-Former-based approach. These results suggest that though our method is designed to create new interactive ways instead of focusing on bench-

method	MMBench-dev							MMBench-test						
	Overall	LR	AR	RR	FP-S	FP-C	CP	Overall	LR	AR	RR	FP-S	FP-C	CP
MMICL [50]	67.9	49.2	71.6	73.0	66.7	57.2	77.2	65.2	44.3	77.9	64.8	66.5	53.6	70.6
mPLUG-Owl2 [14]	66.5	32.2	72.4	60.9	68.6	60.1	79.4	66.0	<u>43.4</u>	76.0	62.1	68.6	55.9	73.0
Sphinx [51]	67.2	33.1	67.3	58.3	74.4	59.4	<u>80.7</u>	<u>67.5</u>	32.9	73.6	57.8	<u>72.1</u>	63.2	79.2
LLaVA-v1.5 [23]	67.7	41.7	69.7	63.5	70.0	59.3	80.2	67.0	39.9	74.7	61.6	70.9	59.9	75.4
+ Prompt Highlighter	69.7	<u>44.2</u>	70.6	<u>68.7</u>	<u>73.7</u>	<u>59.3</u>	80.9	69.5	42.6	<u>77.5</u>	<u>64.3</u>	75.0	<u>62.0</u>	<u>76.4</u>
Improvement	+2.0	+2.5	+0.9	+5.2	+3.7	0.0	+0.7	+2.5	+2.7	+2.8	+2.7	+4.1	+2.1	+1.0

Table 6. Detailed comparison in MMBench-dev and MMBench-test [26]. The categories include Logic Reasoning (LR), Attribute Reasoning (AR), Relation Reasoning (RR), Instance-Level Fine-Grained Perception (FP-S), Cross-Instance Fine-Grained Perception (FP-C), and Coarse Perception (CP). The improvement of our method over the LLaVA-v1.5 [23] baseline is reported in the last row for each category. We highlight **the best** and underline the second best result for each column.

method	MME	MMB _{dev}	MMB _{test}
LLaVA-v1.5 [23]	1531.3	67.7	67.0
PH (0.01, 3.0 , 1.3)	1537.3	69.7	68.7
PH (0.01, 2.0 , 1.3)	1552.5	68.7	69.5
PH (submitted)	1552.5	70.1	70.7

Table 7. Hyper-parameter settings in VLM benchmarks. Evaluations are conducted on MME Perception [27] and MMBench (MMB) [26]. We list a combination of hyper-parameters (α, β, γ) for our method (PH for Prompt Highlighter).

sub-task	baseline	preference
Text Partial Highlighter	Vicuna-13B	70.6%
Image Partial Highlighter	LLaVA	74.5%
Image Understanding	InstructBLIP	76.5%
Image Caption	LLaVA-v1.5	80.4%
Description \rightarrow Image	LLaVA-v1.5 + DALLE-3	84.3%
Overall	-	77.3%

Table 8. A fine-grained user study result.

mark improvement, it still proves to be competitive in general applications.

A.2.2 Reliable Descriptions

As discussed in Sec. 4.4, we observe a trade-off between the attention concentration and QA performance that appeared in the benchmarks. Therefore, compared with experiments in VLM benchmarks, we adopt a relatively more aggressive parameter setting in the MSCOCO caption experiment: $(\alpha, \beta, \gamma) = (0.01, 7.0, 2.0)$. We utilize a CLIP ViT-Base-32 model [30, 52] to test the CLIP Score [48] and to extract embeddings for both text \rightarrow image and image \rightarrow text retrieval metrics. Our experiment uses a simple input prompt, 'Describe this image.'. In the comparison in Tab. 2, we report the official result reported by CoCa-CFG [22] with the same γ value of 2.0¹. As CLIP has a maximum token length limitation of 77, we split captions at semicolons and periods and input the longest possible concatenated sequence to circumvent this limitation. For all text-to-image generation results in figures, we query the generated text description to the Bing Image Creator powered by DALLE-3 [44] [www.bing.com/images/create].

¹CoCa-CFG achieves caption \rightarrow image retrieval recall with R@1=49.4 and R@5=75.7 with $\gamma = 3.0$, while it remains the same S-CLIP=0.808.

A.2.3 User Study

We present the detailed results of the user study in Tab. 8. Using different sub-task examples, we engaged various baseline models for different tasks to demonstrate the consistent preference for Prompt Highlighter across a broad array of frameworks and tasks. The user preference results affirm that our method delivers superior performance and flexibility, consistently outperforming the baseline models across a wide range of tasks.

A.3. Attention Map Visualization

In this section, we delve into the attention map visualization, expanding on the verification experiments discussed in Sec. 4.5. In Fig. 10, we illustrate an example akin to Fig. 3, demonstrating the persistence of the band-like pattern in different layer segments in the Vicuna-13B model [8]. The band-like property is clear and consistently evident across various layers. Given that these band-like token activation patterns are distributed across different layers, we simply incorporate the attention activation modification in all self-attention layers. Furthermore, the attention maps referenced in Fig. 9 to calculate gradients and attention contributions are computed based on the averaged attention map across layers and heads.

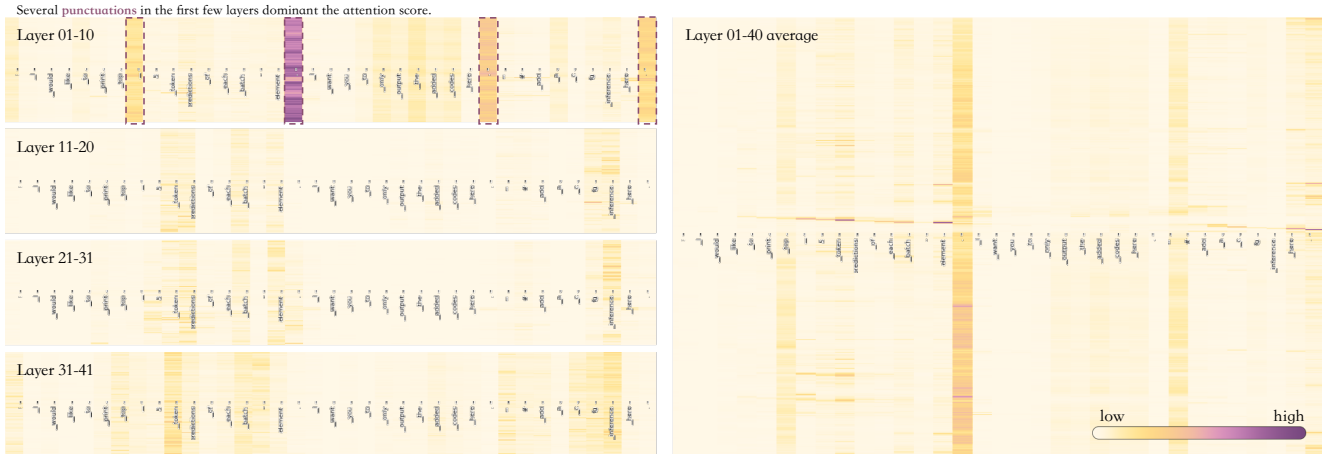


Figure 10. An additional example of attention maps across different layer segments (*left*) and the averaged visualization with more generated tokens (*right*). We mark tokens representing punctuation, which draw significant attention in the initial layers. Beyond these tokens, a consistent correlation between tokens forms a band-like pattern that can be observed across all layers.

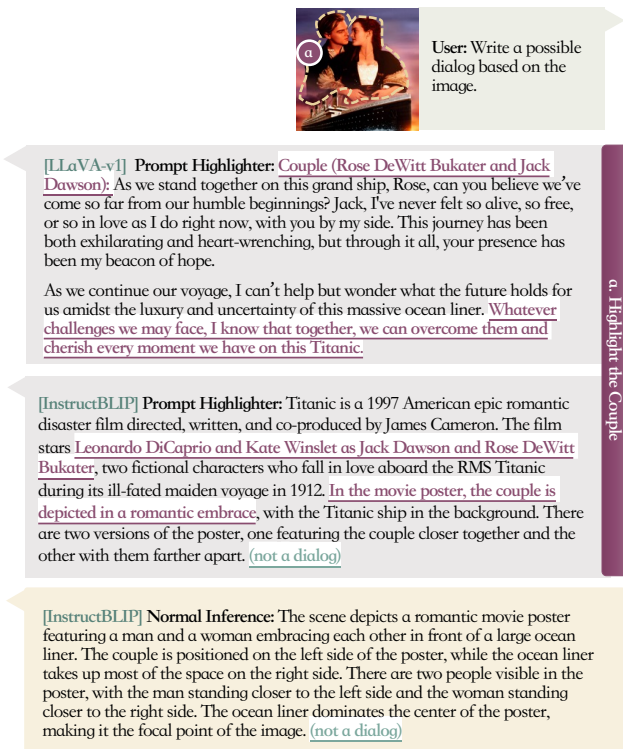


Figure 11. An example illustrating the influence of different base models. Given the same highlighted context, the output of the model may be constrained by the capabilities of the base model.

A.4. Limitation Analysis

A.4.1 Speed and Memory

For processing two tokens compared to single-beam (greedy) inference in image description, batched inference

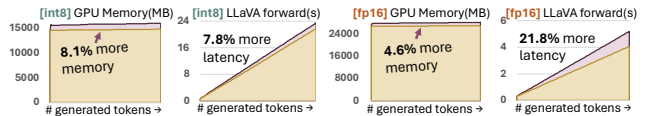


Figure 12. Speed and memory overhead analysis. We evaluate VLM inference both in int8 and fp16 precision.

enables parallel computation, adding only 7% and 10% to the memory and speed costs, respectively. We corroborate this with plotted relation curves for processing $N = 0, \dots, 140$ tokens, demonstrating that our method maintains controllability with minimal extra costs.

As discussed in Sec. 4.5, Prompt Highlighter imposes an additional computational load on the unconditional branch, and we validate its tangible impact in Tab. 5. Memory consumption with 8-bit loading confirms that the Prompt Highlighter is designed to be memory-efficient, making it feasible to run inference on a 13B model using commonly available GPUs, such as the NVIDIA-3090. This added load becomes noticeable when evaluating single-token prediction tasks, as the model is required to compute double KV values among tokens in its initial inference step. However, when employing KV-cache in the multiple-token generation, this extra load can be alleviated, as the doubled calculation with cached KVs does not become the bottleneck for inference speed or GPU memory consumption.

For processing two tokens compared to single-beam (greedy) inference in image description, batched inference enables parallel computation, adding only 7% and 10% to the memory and speed costs, respectively. We corroborate this with plotted relation curves in Fig. 12 for processing $N = 0, \dots, 140$ tokens, demonstrating that our method maintains controllability with minimal extra costs. We also

User: Please give me a plan to learn about `computer vision`.

[Vicuna] Normal Inference:
 1. Start with the basics... 2. Learn about image processing...
 3. Learn a programming language... 4. Learn about OpenCV...
 5. Learn about deep learning... 6. Practice with projects...
 7. Read books and articles... 8. Join online communities...

LLM-CFG:
 1. Learn the basics of programming ... 2. Learn the basics of image processing ... 3. Learn about OpenCV ... 4. Learn about machine learning ... 5. Learn about computer vision algorithms ... 6. Practice with datasets ... 7. Build projects ... 8. Stay up to date ...

Prompt Highlighter:
 1. Foundations of Computer Vision... 2. Image Processing...
 3. Feature Detection... 4. Object Detection... 5. Image Segmentation... 6. Deep Learning for Computer Vision...

Figure 13. One example of the comparison with LLM-CFG [21].

[Vicuna] Please give me a plan to learn about `computer vision`.

$\alpha > 0.1$ Sure, here's a plan to help you learn `computer vision`...

$\alpha = 0.01$ Certainly! Here's a plan to help you `learn Python`...

LLM-CFG Certainly! Here's a plan to help you `learn ASSTST`...

Figure 14. Output example for the unconditional branch with different unconditional context designs.

confirm that the commonly utilized inference strategy of introducing an extra beam search branch does not impair the quality of the descriptive task (S-CLIP 0.809→0.807 in Tab. 5), despite imposing an additional computational load. This also illustrates the practical effectiveness of Prompt Highlighter.

A.4.2 Constrained by the Base-Model

Our method stems from the base model and its plug-and-play nature. As illustrated in Fig. 11, the base model InstructBLIP [15] is not adept at dialog generation. Consequently, with a highlighted prompt context, despite the output text being more related to the highlighted part, it fails to generate a dialogue effectively. This suggests that while the Prompt Highlighter can augment existing abilities in pre-trained multi-modal LLMs, it cannot endow them with new capabilities.

B. Additional Discussions

B.1. Compare with LLM-CFG

The comparison between Prompt Highlighter and LLM-CFG [21] is visually demonstrated in Fig. 13. Our method

User: `<marked_image>` Describe this image, emphasize the marked area.

Normal Inference (add marks and arrow): The image features a man wearing a red and green soccer jersey, smiling and posing for the camera. He is wearing a wristband on his left wrist, and his shirt is numbered with the number seven. The man is standing in a room, possibly a locker room, with a few other people in the background. The main focus of the image is the man in the red and green soccer jersey, and a red arrow is pointing towards him, drawing attention to his presence in the scene.



User: `<original_image>` Describe this image, and emphasize more on the jersey

Normal Inference (prompt engineering): The image features a man wearing a red and green soccer jersey, smiling and posing for the camera. The jersey has a distinctive design, with a combination of red and green colors, and the number seven displayed on it. The man appears to be a soccer player, possibly a professional athlete, as he is wearing a sports uniform and is in a stadium setting.

User: `<masked_image>` Describe this image

Normal Inference (physically "highlight" the jersey part and input a masked image): The image features a man wearing a red and green soccer jersey, standing on a field and smiling. He appears to be a soccer player, possibly a professional athlete, as he is wearing a uniform and is in a stadium setting. The man is the main focus of the image, and he is surrounded by a crowd of people, indicating that he might be participating in a game or event.



User: `< original_image, m>` Describe this image

Prompt Highlighter: The image features a soccer player wearing a red, green, and gold jersey with the number 7 on it. The player is smiling and appears to be enjoying the game. He is wearing green and red stripes on his jersey, which are visible on the sleeves and the green stripe on the side. The player is also wearing a green and white armband on his right arm. The scene captures the excitement and enthusiasm of the soccer player as he participates in the game.

Figure 15. A comparison of Prompt Highlighter with different vision-language prompt manipulation approaches.

stands out by offering a more granular control mechanism that allows specific tokens within the context to be highlighted. Conversely, LLM-CFG, with its basic prompt-level differentiation and without a mechanism to directly manipulate model feature interactions (e.g., our attention activation strategy), often generates outputs that bear noticeable similarity to the original, regardless of substantial γ increases.

Using the identical prompt as in Fig. 13, we consolidate this claim by exhibiting the independent inference outcomes of the unconditional branch in Fig. 14. In addition, we demonstrate the significance of assigning the α value at the embedding layer. As shown in Fig. 14 and as per our discussion in Sec. 3.1, it becomes apparent that a small scalar multiplication α in the embedding space leaves the overall contextual understanding of the unconditional branch largely unaffected. Such a fine-grained difference assists in making more distinguishing token choices during the inference process in Eq. (6). In contrast, LLM-CFG’s unconditional

branch omits part of the prompt, resulting in an obstacle to generating results that effectively underscore the highlighted sections.

B.2. Compare with other Highlight Methods

To demonstrate the non-trivial nature of our method, we evaluated it alongside several intuitive prompt engineering approaches, which include adding adjectives, capitalizing text, and explicitly marking in images. Comparative examples in LLM and VLM are provided in Figs. 1 and 15, respectively. Our observations suggest that the employment of additional prompts or explicit emphasis can occasionally lead to unpredictable results. This is primarily due to the introduction of extra information, while models may not truly emphasize correlated parts. In contrast, our method seamlessly accommodates all context information and produces focused text outputs. This demonstrates that the design of our method not only offers a high degree of flexibility but also enables the generation of more contextually appropriate outputs.

B.3. Highlighting the Whole Image.

We demonstrate in Algorithm 2 and Sec. 3.2 that self-generated tokens may lead to model hallucinations. The model’s attention is steered towards trustworthy content by purposefully highlighting the reliable input context, such as the entire image, mitigating hallucinations in extended text generation. An example from MME is provided below to show how this approach effectively curbs hallucinations during evaluations.



Figure 19. An example of highlighting image context to eliminate hallucination.

C. Showcases

C.1. More Visual Results

Additional results of Prompt Highlighter in LLM and VLM are provided in Fig. 16 and Fig. 17, respectively.

In the first example of Fig. 16, we showcase the primary part of the output of the example in Fig. 6. Our results concentrate more on the highlighted section, offering professional reference books to support user learning “computer vision”. The second example exhibits a case for a multi-segment mask input, where the model is steered to output code snippets at the appropriate positions by highlighting the requirement part of the text and the comment as the position identifier. Fig. 17 demonstrates a range of applications and capabilities of Prompt Highlighter in VLM from various perspectives, including image content comprehension

(case 1), focused generation (case 2), improved image descriptions (case 3), and explicit generation control (case 5). These instances underscore the performance enhancement and customizable generation control facilitated by Prompt Highlighter. We also present some challenging cases due to the limited perceptual capacity of the base model.

Moreover, we present results of text-to-image generation based on the text descriptions generated by our method in Fig. 18. These outcomes vouch for the superior capability of our approach in descriptive tasks and its proficiency in generating higher-quality image-text matching data.

C.2. Multi-Round Interactive Conversation

Up to this point, the examples and experimental scenarios we’ve showcased are for single-round dialogues or QAs. As a general-purpose interactive inference pipeline, our method can also support multi-round interactions and conversations. We provide a schematic diagram of multi-round conversation at the top of Fig. 20. The multi-round conversations’ generation can be decomposed into single-round generations with continuously growing context, allowing Prompt Highlighter to change the focus of user input in each round by updating the input mask m and resetting previous KV caches.

Below the pipeline, we demonstrate how to resolve the image understanding problem, presented in Fig. 17 case 4, through multi-round conversation and human interactions. By highlighting multi-modal tokens and guiding the model to understand the image content in a segmented manner, users can “teach” the model to solve problems that it was previously unable to solve.

Figures 15-18 are presented on the following pages ↓

Case1: A full version of the first example in Fig. 6 Normal Inference Prompt Highlighter

User: Please give me a plan to learn about computer vision.

1. Start with the basics: Before diving into the advanced concepts of computer vision, it's essential to have a solid understanding of the fundamentals. Learn about the different types of computer vision, such as object recognition, image segmentation, and motion analysis.
2. Learn about image processing: Image processing is a crucial aspect of computer vision. Learn about image filtering, edge detection, and other image processing techniques.
3. Learn a programming language: Python is the most popular language used in computer vision. Learn the basics of Python and familiarize yourself with the libraries commonly used in computer vision, such as OpenCV, TensorFlow, and Keras.
4. Learn about OpenCV: OpenCV is a powerful library for computer vision tasks. Learn about its various functions and how to use them to implement computer vision algorithms.
5. Learn about deep learning: Deep learning is a subset of machine learning that uses neural networks to perform tasks. Learn about the basics of deep learning and how it's used in computer vision.
6. Practice with projects: The best way to learn computer vision is by practicing with projects. Start with simple projects and work your way up to more complex ones. This will help you apply what you've learned and improve your skills.
7. Read books and articles: There are many books and articles available on computer vision. Read them to learn about the latest developments in the field and to gain a deeper understanding of the concepts.
8. Join online communities: Join online communities, such as forums and social media groups, to connect with other computer vision enthusiasts. This will help you learn from others and stay up-to-date with the latest developments in the field.

1. Foundations of Computer Vision: Start by learning the basics of computer vision, including image processing, feature detection, and image matching. Read books like "Computer Vision: Algorithms and Applications" by Richard Szeliski and "Introduction to Computer Vision" by Richard Szeliski, et al.
2. Image Processing: Learn image processing techniques such as filtering, thresholding, and edge detection. Read books like "Image Processing: The Fundamentals" by John C. Bovik and "Digital Image Processing" by Rafael C. Gonzalez and Richard E. Woods.
3. Feature Detection: Learn about feature detection techniques such as SIFT, SURF, and ORB. Read papers like "SIFT: Scale-Invariant Feature Transform" by David G. Lowe and "ORB: Oriented FAST and Rotated BRIEF SIFT" by Yi Liu and Aki Kanade.
4. Object Detection: Learn about object detection techniques such as Haar cascades, HOG, and Viola-Jones algorithms. Read papers like "Haar Cascades for Real-Time Object Detection" by Andreas Santner, et al. and "A Survey of Object Detection" by Paul Viola and Michael Jones.
5. Image Segmentation: Learn about image segmentation techniques such as connected component analysis, region growing, and watershed segmentation. Read books like "Image Segmentation: Algorithms and Applications" by T. P. Singh and "Computer Vision: A Modern Approach" by David A. Forsyth and Jean Ponce.
6. Deep Learning for Computer Vision: Learn about deep learning techniques for computer vision, including convolutional neural networks (CNNs) and recurrent neural networks (RNNs). Read books like "Deep Learning for Computer Vision" by Rajalingapuram Kannan and "Computer Vision with Deep Learning" by S. S. K. Tiwari and S. C. Gupta.
7. Practice and Projects: Practice your computer vision skills by working on projects and datasets such as ImageNet, OpenCV, and Kaggle.

Case2: Specific requirement in code generation. We partial highlight both the text prompt and the position comment in the code segment.

```
# add a cfg inference here.
def CFG_greedy_forward(input, model, guidance=1.5, max_length=256):
    new_ids = [1]
    for i in tqdm(range(max_length)):
        if i == 0: # update the augmented key-values
            dict_outputs = model(inputs_embeds=input, past_key_values=key_values, return_dict=True)
        else:
            dict_outputs = model(inputs_embeds=input, return_dict=True, use_cache=True, output_attentions=True)

        last_logits = torch.argmax(dict_outputs.logits[:, -1:], dim=-1)
        # INSERT CODE HERE
        new_ids += [last_logits]
        if last_logits == 2: # stop token.
            break
        last_logits_embed = model.get_input_embeddings()(last_logits)
        input = torch.cat((input, last_logits_embed), dim=1)
        cfg_batched_input = torch.cat([embed, highlighted_embed])
```

User: I would like to print top 5 token predictions of last_logits. Directly output the newly added codes.

You can simply print the top 5 token predictions of the last logit by sorting the logits in descending order and taking the first 5 elements. Here's the updated code:

```
# add a cfg inference here.
def CFG_greedy_forward(input, model, guidance=1.5, max_length=256):
    new_ids = [1]
    for i in tqdm(range(max_length)):
        if i == 0: # update the augmented key-values
            dict_outputs = model(inputs_embeds=input, past_key_values=key_values, return_dict=True)
        else:
            dict_outputs = model(inputs_embeds=input, return_dict=True, use_cache=True, output_attentions=True)
        last_logits = torch.argmax(dict_outputs.logits[:, -1:], dim=-1)
        # INSERT CODE HERE
        new_ids += [last_logits]
        if last_logits == 2: # stop token.
            break
        last_logits_embed = model.get_input_embeddings()(last_logits)
        input = torch.cat((input, last_logits_embed), dim=1)
        cfg_batched_input = torch.cat([embed, highlighted_embed])
        return cfg_batched_input

    # sort the logits in descending order and take the first 5 elements
    logits = dict_outputs.logits[:, -1:]
    sorted_logits = logits.sort(desc=True)[:5]

    # print the top 5 token predictions
    print(sorted_logits)
```

Here's the added part to print the top 5 token predictions of the last logit:

```
# INSERT CODE HERE
top_tokens = sorted(last_logits, key=lambda x: dict_outputs.logits[0, x], reverse=True)[:5]
print(top_tokens)
```

This code sorts the last logit based on the logits and selects the top 5 tokens. The logits represent the model's confidence in each token being the next one in the sequence, so the top 5 tokens with the highest logits are likely to be the correct predictions. Finally, the code prints the added part.

Figure 16. Two more examples in pure text partial highlighter. A Vicuna-13B-v1.1 [8] is used as the base model.

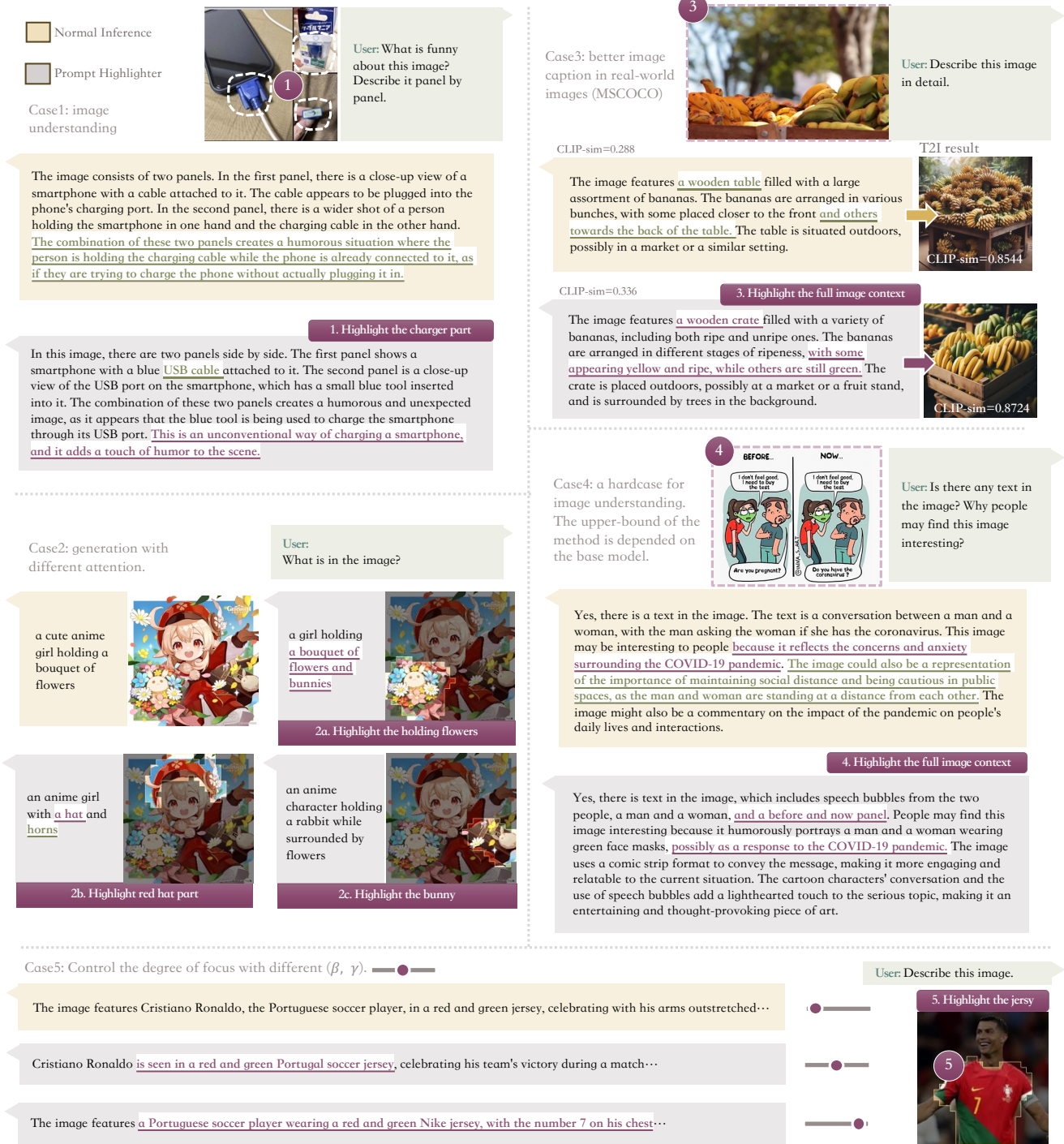
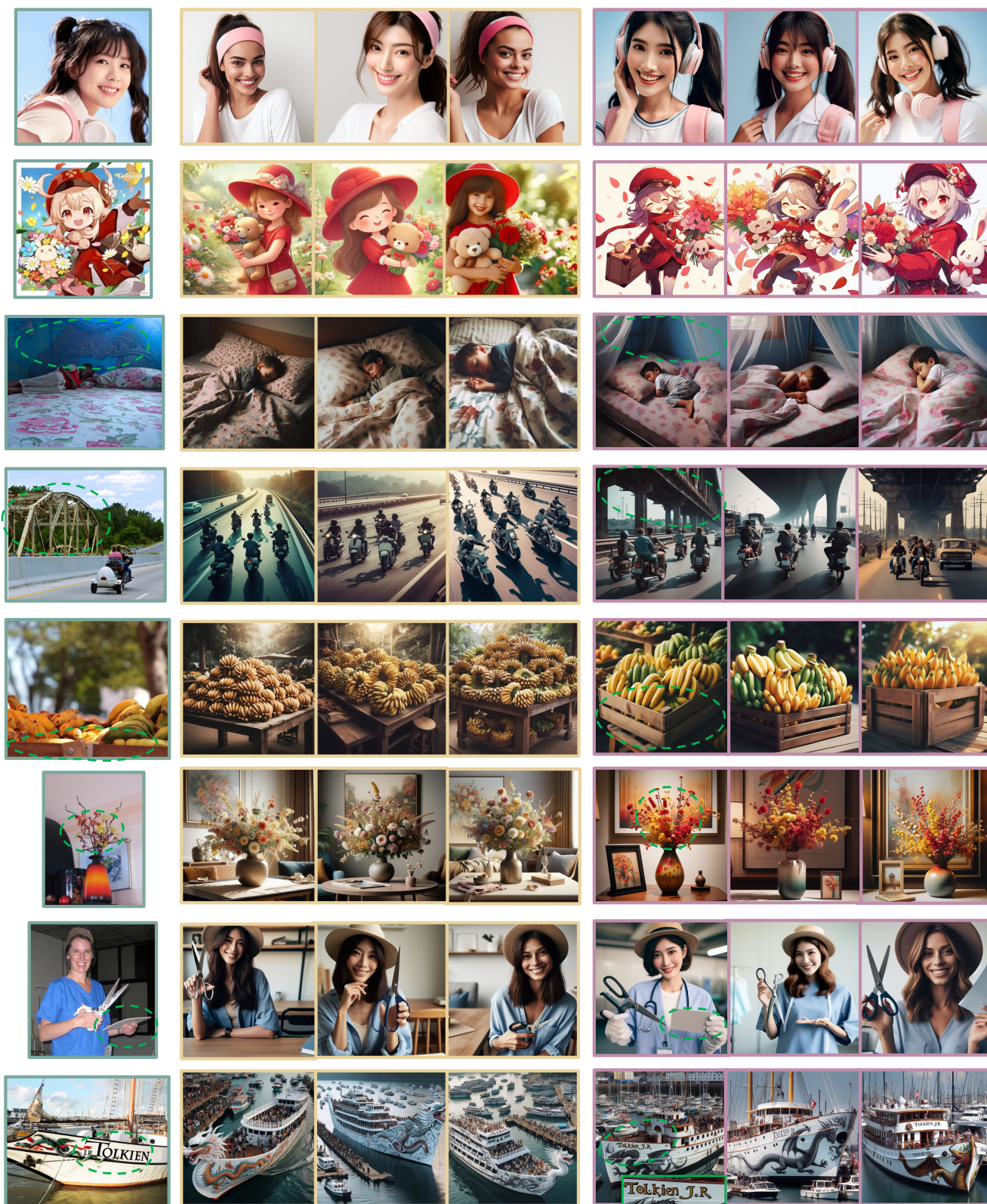


Figure 17. More results with multi-modal inputs. We demonstrate three applications (1,2,3,5) and one hard case (4) for image understanding. We use InstructBLIP-Vicuna-13B [15] as the base model of cases 1,2,5 and LLaVA-v1.5 [23] 13B as the base model of cases 3,4.



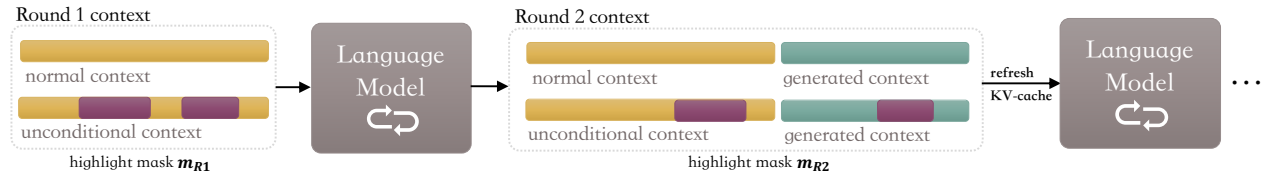
Input images

T2I results using text from vanilla inference

T2I results using text from context-highlighted inference

Figure 18. More text-to-image examples with image generation by DALLE-3 [44]. We have marked areas in some figures that generate better results due to different captions.

Multi-Round Conversation



Vanilla inference

BEFORE... I don't feel good, need to see the test? Do you have the coronavirus?
NOW... I don't feel good, need to see the test? Do you have the coronavirus?

Round 1
 User: <image> Describe the conversation in the left side image.
 Assistant: In the left side image, a man and a woman are having a conversation. The woman is wearing a green face mask, and the man is wearing a green neck gaiter. They are talking about the coronavirus, with the woman possibly expressing her concerns or sharing information about the virus. The man is listening attentively to the woman's words.

Round 2
 User: Describe the conversation in the right side of the image, then try to explain the meme inside the image.
 Assistant: In the right side of the image, a man and a woman are having a conversation. The woman is wearing a green face mask, and the man is wearing a green neck gaiter. They are talking about the coronavirus, with the woman possibly expressing her concerns or sharing information about the virus. The meme inside the image is a play on the idea of a "before" and "after" scenario. The "before" scenario shows the man and woman talking about the coronavirus, while the "after" scenario shows the same man and woman talking about the same topic, but with the woman wearing a green face mask and the man wearing a green neck gaiter. This meme is likely meant to emphasize the importance of wearing face masks and practicing social distancing to prevent the spread of the virus.

Interactive Inference

BEFORE... I don't feel good, need to see the test? Do you have the coronavirus?
NOW... I don't feel good, need to see the test? Do you have the coronavirus?

Round 1
 User: <image> Describe the conversation in the left side image.
 Assistant: In the left side image, the conversation between the two people is about pregnancy. The woman is talking to the man, who is wearing a green face mask, and asking him if he is pregnant. The man is responding by saying, "Are you are you pregnant?". This conversation is taking place in a setting where the woman is wearing a green face mask, and the man is wearing a green face mask as well.

Round 2
 User: Describe the conversation in the right side of the image, then try to explain the meme inside the image.
 Assistant: In the right side of the image, the conversation is about the coronavirus. The woman is talking to the man, who is wearing a green face mask, and asking him if he has the coronavirus. The man is responding by saying, "Do you have the coronavirus?". This conversation is taking place in a setting where both the woman and the man are wearing green face masks. The meme inside the image is a play on words, using the phrase "now" to represent the present time and the phrase "before" to represent the past. The two conversations are juxtaposed, with the left side showing a pregnancy-related conversation and the right side showing a conversation about the coronavirus. The meme is a creative way to compare and contrast two different situations and their respective concerns.

Figure 20. Multi-round interactive conversation powered by Prompt Highlighter. We illustrate the multi-round interactive conversation pipeline on the *top*. We provide a comparison in a multi-round conversation between the vanilla inference (*left*) and Prompt Highlighter (*right*). In this example, the user highlights different contexts in two rounds.

References

- [1] Alec Radford, Karthik Narasimhan, Tim Salimans, Ilya Sutskever, et al. Improving language understanding by generative pre-training. 2018. [1](#), [2](#)
- [2] Alec Radford, Jeffrey Wu, Rewon Child, David Luan, Dario Amodei, Ilya Sutskever, et al. Language models are unsupervised multitask learners. *OpenAI blog*, 1(8):9, 2019.
- [3] Tom Brown, Benjamin Mann, Nick Ryder, Melanie Subbiah, Jared D Kaplan, Prafulla Dhariwal, Arvind Neelakantan, Pranav Shyam, Girish Sastry, Amanda Askell, et al. Language models are few-shot learners. *NeurIPS*, 33:1877–1901, 2020.
- [4] Yinhan Liu, Myle Ott, Naman Goyal, Jingfei Du, Mandar Joshi, Danqi Chen, Omer Levy, Mike Lewis, Luke Zettlemoyer, and Veselin Stoyanov. Roberta: A robustly optimized bert pretraining approach. *arXiv preprint arXiv:1907.11692*, 2019.
- [5] Jacob Devlin, Ming-Wei Chang, Kenton Lee, and Kristina Toutanova. Bert: Pre-training of deep bidirectional transformers for language understanding. *arXiv preprint arXiv:1810.04805*, 2018.
- [6] Mike Lewis, Yinhan Liu, Naman Goyal, Marjan Ghazvininejad, Abdelrahman Mohamed, Omer Levy, Ves Stoyanov, and Luke Zettlemoyer. Bart: Denoising sequence-to-sequence pre-training for natural language generation, translation, and comprehension. *arXiv preprint arXiv:1910.13461*, 2019.
- [7] Hugo Touvron, Thibaut Lavril, Gautier Izacard, Xavier Martinet, Marie-Anne Lachaux, Timothée Lacroix, Baptiste Rozière, Naman Goyal, Eric Hambro, Faisal Azhar, et al. Llama: Open and efficient foundation language models. *arXiv preprint arXiv:2302.13971*, 2023. [2](#), [4](#), [5](#)
- [8] Wei-Lin Chiang, Zhuohan Li, Zi Lin, Ying Sheng, Zhanghao Wu, Hao Zhang, Lianmin Zheng, Siyuan Zhuang, Yonghao Zhuang, Joseph E Gonzalez, et al. Vicuna: An open-source chatbot impressing gpt-4 with 90%* chatgpt quality. See <https://vicuna.lmsys.org> (accessed 14 April 2023), 2023. [4](#), [5](#), [10](#), [14](#)
- [9] Hyung Won Chung, Le Hou, Shayne Longpre, Barret Zoph, Yi Tay, William Fedus, Eric Li, Xuezhi Wang, Mostafa Dehghani, Siddhartha Brahma, et al. Scaling instruction-finetuned language models. *arXiv preprint arXiv:2210.11416*, 2022. [1](#), [2](#)
- [10] Haotian Liu, Chunyuan Li, Qingyang Wu, and Yong Jae Lee. Visual instruction tuning. *arXiv preprint arXiv:2304.08485*, 2023. [1](#), [2](#), [4](#), [5](#)
- [11] Deyao Zhu, Jun Chen, Xiaoqian Shen, Xiang Li, and Mohamed Elhoseiny. Minigt-4: Enhancing vision-language understanding with advanced large language models. *arXiv preprint arXiv:2304.10592*, 2023. [2](#), [4](#)
- [12] Junnan Li, Dongxu Li, Caiming Xiong, and Steven Hoi. Blip: Bootstrapping language-image pre-training for unified vision-language understanding and generation. In *ICML*, pages 12888–12900. PMLR, 2022.
- [13] Junnan Li, Dongxu Li, Silvio Savarese, and Steven Hoi. Blip-2: Bootstrapping language-image pre-training with frozen image encoders and large language models. *arXiv preprint arXiv:2301.12597*, 2023. [2](#), [4](#)
- [14] Qinghao Ye, Haiyang Xu, Guohai Xu, Jiabo Ye, Ming Yan, Yiyang Zhou, Junyang Wang, Anwen Hu, Pengcheng Shi, Yaya Shi, et al. mplug-owl: Modularization empowers large language models with multimodality. *arXiv preprint arXiv:2304.14178*, 2023. [4](#), [7](#), [10](#)
- [15] Wenliang Dai, Junnan Li, Dongxu Li, Anthony Meng Huat Tiong, Junqi Zhao, Weisheng Wang, Boyang Li, Pascale Fung, and Steven Hoi. Instructblip: Towards general-purpose vision-language models with instruction tuning, 2023. [1](#), [2](#), [5](#), [12](#), [15](#)
- [16] Shunyu Yao, Dian Yu, Jeffrey Zhao, Izhak Shafran, Thomas L Griffiths, Yuan Cao, and Karthik Narasimhan. Tree of thoughts: Deliberate problem solving with large language models. *arXiv preprint arXiv:2305.10601*, 2023. [1](#), [2](#)
- [17] Jason Wei, Xuezhi Wang, Dale Schuurmans, Maarten Bosma, Fei Xia, Ed Chi, Quoc V Le, Denny Zhou, et al. Chain-of-thought prompting elicits reasoning in large language models. *NeurIPS*, 35:24824–24837, 2022. [2](#)
- [18] Significant-Gravitas. Significant-gravitas/autogpt: An experimental open-source attempt to make gpt-4 fully autonomous. [2](#)
- [19] Xuezhi Wang, Jason Wei, Dale Schuurmans, Quoc Le, Ed Chi, Sharan Narang, Aakanksha Chowdhery, and Denny Zhou. Self-consistency improves chain of thought reasoning in language models. *arXiv preprint arXiv:2203.11171*, 2022. [1](#), [2](#)
- [20] Jonathan Ho and Tim Salimans. Classifier-free diffusion guidance. *arXiv preprint arXiv:2207.12598*, 2022. [2](#), [3](#)
- [21] Guillaume Sanchez, Honglu Fan, Alexander Spangher, Elad Levi, Pawan Sasanka Ammanamanchi, and Stella Biderman. Stay on topic with classifier-free guidance. *arXiv preprint arXiv:2306.17806*, 2023. [3](#), [5](#), [8](#), [12](#)
- [22] Simon Kornblith, Lala Li, Zirui Wang, and Thao Nguyen. Guiding image captioning models toward more specific captions. In *ICCV*, pages 15259–15269, 2023. [2](#), [7](#), [10](#)
- [23] Haotian Liu, Chunyuan Li, Yuheng Li, and Yong Jae Lee. Improved baselines with visual instruction tuning. *arXiv preprint arXiv:2310.03744*, 2023. [2](#), [5](#), [7](#), [9](#), [10](#), [15](#)
- [24] Rohan Bavishi, Erich Elsen, Curtis Hawthorne, Maxwell Nye, Augustus Odena, Arushi Somani, and Sağnak Taşlılar. Introducing our multimodal models, 2023. [2](#)
- [25] Tsung-Yi Lin, Michael Maire, Serge Belongie, James Hays, Pietro Perona, Deva Ramanan, Piotr Dollár, and C Lawrence Zitnick. Microsoft coco: Common objects in context. In *ECCV*, pages 740–755. Springer, 2014. [2](#), [7](#)
- [26] Yuan Liu, Haodong Duan, Yuanhan Zhang, Bo Li, Songyang Zhang, Wangbo Zhao, Yike Yuan, Jiaqi Wang, Conghui He, Ziwei Liu, et al. Mmbench: Is your multi-modal model an all-around player? *arXiv preprint arXiv:2307.06281*, 2023. [2](#), [6](#), [7](#), [10](#)
- [27] Chaoyou Fu, Peixian Chen, Yunhang Shen, Yulei Qin, Mengdan Zhang, Xu Lin, Zhenyu Qiu, Wei Lin, Jinrui Yang, Xiwu Zheng, et al. Mme: A comprehensive evaluation benchmark for multimodal large language models. *arXiv preprint arXiv:2306.13394*, 2023. [2](#), [6](#), [7](#), [10](#)
- [28] Hugo Touvron, Louis Martin, Kevin Stone, Peter Albert, Amjad Almahairi, Yasmine Babaei, Nikolay Bashlykov,

- Soumya Batra, Prajjwal Bhargava, Shruti Bhosale, et al. Llama 2: Open foundation and fine-tuned chat models. *arXiv preprint arXiv:2307.09288*, 2023. 2
- [29] Aakanksha Chowdhery, Sharan Narang, Jacob Devlin, Maarten Bosma, Gaurav Mishra, Adam Roberts, Paul Barham, Hyung Won Chung, Charles Sutton, Sebastian Gehrmann, et al. Palm: Scaling language modeling with pathways. *arXiv preprint arXiv:2204.02311*, 2022.
- [30] Alec Radford, Jong Wook Kim, Chris Hallacy, Aditya Ramesh, Gabriel Goh, Sandhini Agarwal, Girish Sastry, Amanda Askell, Pamela Mishkin, Jack Clark, et al. Learning transferable visual models from natural language supervision. In *ICML*, pages 8748–8763. PMLR, 2021. 2, 7, 10
- [31] Zhiliang Peng, Wenhui Wang, Li Dong, Yaru Hao, Shaohan Huang, Shuming Ma, and Furu Wei. Kosmos-2: Grounding multimodal large language models to the world. *arXiv preprint arXiv:2306.14824*, 2023. 2
- [32] Pan Zhang, Xiaoyi Dong, Bin Wang, Yuhang Cao, Chao Xu, Linke Ouyang, Zhiyuan Zhao, Shuangrui Ding, Songyang Zhang, Haodong Duan, Wenwei Zhang, Hang Yan, Xinyue Zhang, Wei Li, Jingwen Li, Kai Chen, Conghui He, Xingcheng Zhang, Yu Qiao, Dahua Lin, and Jiaqi Wang. Internlm-xcomposer: A vision-language large model for advanced text-image comprehension and composition, 2023. 2, 9
- [33] Maciej Besta, Nils Blach, Ales Kubicek, Robert Gerstenberger, Lukas Gianinazzi, Joanna Gajda, Tomasz Lehmann, Michal Podstawski, Hubert Niewiadomski, Piotr Nyczyk, et al. Graph of thoughts: Solving elaborate problems with large language models. *arXiv preprint arXiv:2308.09687*, 2023. 2
- [34] Yuxi Xie, Kenji Kawaguchi, Yiran Zhao, Xu Zhao, Min-Yen Kan, Junxian He, and Qizhe Xie. Decomposition enhances reasoning via self-evaluation guided decoding. *arXiv preprint arXiv:2305.00633*, 2023. 2
- [35] Wei-Ge Chen, Irina Spiridonova, Jianwei Yang, Jianfeng Gao, and Chunyuan Li. Llava-interactive: An all-in-one demo for image chat, segmentation, generation and editing, 2023. 2
- [36] Xin Lai, Zhuotao Tian, Yukang Chen, Yanwei Li, Yuhui Yuan, Shu Liu, and Jiaya Jia. Lisa: Reasoning segmentation via large language model. *arXiv preprint arXiv:2308.00692*, 2023. 2
- [37] Zeyi Sun, Ye Fang, Tong Wu, Pan Zhang, Yuhang Zang, Shu Kong, Yuanjun Xiong, Dahua Lin, and Jiaqi Wang. Alphaclip: A clip model focusing on wherever you want, 2023. 2
- [38] Songwei Ge, Taesung Park, Jun-Yan Zhu, and Jia-Bin Huang. Expressive text-to-image generation with rich text. In *ICCV*, 2023. 3
- [39] Hila Chefer, Yuval Alaluf, Yael Vinker, Lior Wolf, and Daniel Cohen-Or. Attend-and-excite: Attention-based semantic guidance for text-to-image diffusion models. *arXiv preprint arXiv:2301.13826*, 2023. 3
- [40] David Wan, Jaemin Cho, Elias Stengel-Eskin, and Mohit Bansal. Contrastive region guidance: Improving grounding in vision-language models without training. 2024. 3
- [41] Linxi Zhao, Yihe Deng, Weitong Zhang, and Quanquan Gu. Mitigating object hallucination in large vision-language models via classifier-free guidance, 2024. 3
- [42] Prafulla Dhariwal and Alexander Nichol. Diffusion models beat gans on image synthesis. *NeurIPS*, 34:8780–8794, 2021. 3
- [43] Guangxuan Xiao, Yuandong Tian, Beidi Chen, Song Han, and Mike Lewis. Efficient streaming language models with attention sinks. *arXiv*, 2023. 4
- [44] James Betker, Gabriel Goh, Li Jing, Tim Brooks, Jianfeng Wang, Linjie Li, Long Ouyang, Juntang Zhuang, Joyce Lee, Yufei Guo, Wesam Manassra, Prafulla Dhariwal, Casey Chu, Yunxin Jiao, and Aditya Ramesh. Improving image generation with better captions. Technical report, OpenAI, 2023. 6, 7, 10, 16
- [45] Haotian Liu, Chunyuan Li, Yuheng Li, Bo Li, Yuanhan Zhang, Sheng Shen, and Yong Jae Lee. Llava-next: Improved reasoning, ocr, and world knowledge, January 2024. 6
- [46] Jinze Bai, Shuai Bai, Shusheng Yang, Shijie Wang, Sinan Tan, Peng Wang, Junyang Lin, Chang Zhou, and Jingren Zhou. Qwen-vl: A frontier large vision-language model with versatile abilities. *arXiv preprint arXiv:2308.12966*, 2023. 7
- [47] Noam Rotstein, David Bensaid, Shaked Brody, Roy Ganz, and Ron Kimmel. Fusecap: Leveraging large language models to fuse visual data into enriched image captions. *arXiv preprint arXiv:2305.17718*, 2023. 7
- [48] Jack Hessel, Ari Holtzman, Maxwell Forbes, Ronan Le Bras, and Yejin Choi. Clipscore: A reference-free evaluation metric for image captioning. *arXiv preprint arXiv:2104.08718*, 2021. 6, 10
- [49] Yuechen Zhang, Jinbo Xing, Eric Lo, and Jiaya Jia. Real-world image variation by aligning diffusion inversion chain. In *NeurIPS*, 2023. 8
- [50] Haozhe Zhao, Zefan Cai, Shuzheng Si, Xiaojian Ma, Kaikai An, Liang Chen, Zixuan Liu, Sheng Wang, Wenjuan Han, and Baobao Chang. Mmicl: Empowering vision-language model with multi-modal in-context learning, 2023. 10
- [51] Ziyi Lin, Chris Liu, Renrui Zhang, Peng Gao, Longtian Qiu, Han Xiao, Han Qiu, Chen Lin, Wenqi Shao, Keqin Chen, Jiaming Han, Siyuan Huang, Yichi Zhang, Xuming He, Hongsheng Li, and Yu Qiao. Sphinx: The joint mixing of weights, tasks, and visual embeddings for multi-modal large language models. https://github.com/Alpha-VLLM/LLaMA2-Accessory/blob/main/SPHINX/SPHINX_paper.pdf, 2023. 10
- [52] Alexey Dosovitskiy, Lucas Beyer, Alexander Kolesnikov, Dirk Weissenborn, Xiaohua Zhai, Thomas Unterthiner, Mostafa Dehghani, Matthias Minderer, Georg Heigold, Sylvain Gelly, Jakob Uszkoreit, and Neil Houlsby. An image is worth 16x16 words: Transformers for image recognition at scale. In *ICLR*, 2021. 10